Pekka Alitalo, Olli Luukkonen, Liisi Jylhä, Jukka Venermo, and Sergei A. Tretyakov. 2008. Transmission-line networks cloaking objects from electromagnetic fields. IEEE Transactions on Antennas and Propagation, volume 56, number 2, pages 416-424.

Transmission-Line Networks Cloaking Objects From Electromagnetic Fields

Pekka Alitalo, Olli Luukkonen, Liisi Jylhä, Jukka Venermo, and Sergei A. Tretyakov, *Fellow, IEEE*

***Abstract*—We consider a novel method of cloaking objects from the surrounding electromagnetic fields in the microwave region. The method is based on transmission-line networks that simulate the wave propagation in the medium surrounding the cloaked object. The electromagnetic fields from the surrounding medium are coupled into the transmission-line network that guides the waves through the cloak thus leaving the cloaked object undetected. The cloaked object can be an array or interconnected mesh of small inclusions that fit inside the transmission-line network.**

***Index Terms*—Cloak, dispersion, isotropy, transmission-line network.**

I. Introduction

RECENTLY the subject of cloaking, i.e., reduction of the total scattering cross section of an object, has aroused a lot of interest. Devices capable of cloaking an object from the surrounding electromagnetic fields have been suggested in [1]–[9]. A realization of an electromagnetic cloak operating in the microwave regime has been manufactured and measured [4]. The operation of the cloaks discussed in [1]–[4] is based on mapping of the electromagnetic fields in such a way that the waves that come in contact with the cloak, are guided *around* the object which is placed inside the cylindrical or spherical cloak. The main drawback of the designs presented in [1]–[4] is that these systems are capable of cloaking only from time-harmonic fields, when the object size is comparable to the wavelength. This is because the waves that go around the cloaked object need to go as fast as the wave propagating in free space on a straight line. No object can therefore be fully cloaked from signals because the energy velocity in the (passive) cloak can never exceed the speed of light. Another approach to cloaking objects is based on the cancellation of the dipole moments created by an object by covering it with a plasmonic or a metamaterial coating [5]–[7]. This approach has the drawback of requiring different cloak materials or different thicknesses of the cloak depending on the material properties of the cloaked object (unless this object is placed inside a perfectly conducting enclosure) [5]–[7]. In [8] a way of cloaking polarizable lines or point dipoles situated near a cloak made of a superlens is presented. Yet another approach to design a cloak, based on hard surfaces, was earlier proposed in [9]. This approach has the drawback of strong anisotropy, since the operation of the structure depends strongly on the incidence angle of the illuminating wave.

In this paper we present a novel method for realization of an electromagnetic cloak operating in the microwave region. The operation of the cloak is based on transmission-line (TL) networks which can be unloaded or periodically loaded by lumped elements, such as capacitors and inductors [10], [11]. The cloak itself is composed of these networks and the wave coming from the surrounding medium travels through the cloak inside the transmission-line network (no field mapping is needed). The space between the neighboring transmission lines of the network is left undetected, i.e., cloaked from the electromagnetic fields.

The evident drawback of this approach is that a large bulky object cannot be cloaked due to the periodicity of the transmission-line network. On the other hand, the cloaked object does not have to be composed of tiny pieces that are not in contact with each other, but it can be a three-dimensional mesh of metal or any other material. Also, it is clear that because no field mapping and no exotic material parameters are required, the cloak design and manufacturing are fairly straightforward. Furthermore, if the cloaked object is a mesh of small connected or non-connected objects, cloaking from arbitrary pulses (signal operation) is in principle possible, since instead of going around the object, the waves go *through* the object.

For simplification we consider only a two-dimensional cylindrical cloak here (infinite in the axial direction). However, the same approach can be easily realized also in three dimensions and for arbitrary shapes, while preserving full isotropy of voltage and current waves travelling inside the network, see, e.g., [12]. Because no re-routing of the incident electromagnetic wave around the cloaked object occurs, the current design can be used also as a slab that cloaks an object from an incoming beam. To demonstrate this fact and also the simple realizability of our approach, we present full-wave simulations of a realizable cloak slab.

II. Operation of the Cloak

The cloak that we study in this paper is a two-dimensional simplification of an isotropic three-dimensional cloak, as was also the design realized in [4]. Because the cloak is based on a transmission-line network, it is fairly easy to extend to three dimensions as well: recently the interest in obtaining isotropic TL-based metamaterials for superlensing applications

Manuscript received June 14, 2007; revised August 29, 2007. This work was supported in part by the Academy of Finland and in part by TEKES through the Center-of-Excellence program. The work of P. Alitalo was supported by the Graduate School in Electronics, Telecommunications and Automation (GETA) and the Nokia Foundation and the work of L. Jylhä was supported by theGraduate School in Electronics, Telecommunications and Automation (GETA).

P. Alitalo, O. Luukkonen, and S. A. Tretyakov are with the Radio Laboratory/SMARAD Center of Excellence, TKK Helsinki University of Technology, FI-02015 TKK, Finland (e-mail: pekka.alitalo@tkk.fi).

L. Jylhä and J. Venermo are with the Electromagnetics Laboratory, TKK Helsinki University of Technology, FI-02015 TKK, Finland.

Digital Object Identifier 10.1109/TAP.2007.915469

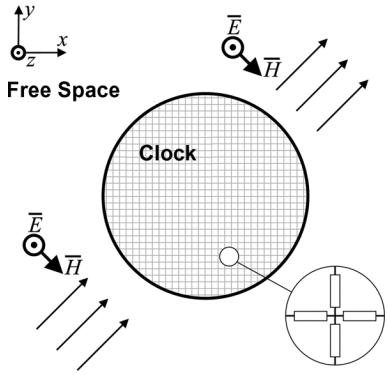

Fig. 1. A two-dimensional cylindrical electromagnetic cloak. The cloak operation does not depend on the incidence angle of the illuminating electromagnetic wave, as long as the network period is small enough with respect to the wavelength.

has resulted in the development of different loaded and unloaded three-dimensional isotropic transmission-line networks [12]–[15].

The cloak design and principle of operation are illustrated in Fig. 1, where a cylindrically shaped cloak (infinite in the z-direction) is placed in free space. The operation and optimization of the properties of the cloak naturally depends on the background medium. In this paper we consider cloaking in free space, as was done in [1]–[9]. The principle of operation is as following: The incident electromagnetic wave in free space arrives to the surface of the cloak, couples into the transmission-line network, and is guided through the cloak that encompasses the object(s) that we want to be hidden. The cloaked object can be a collection of small objects, or it can be a mesh of interconnected objects. The only limitation on the size of the hidden object's inclusions is that they must fit inside the network.

There are two preconditions that have to be met in order that the cloak would operate ideally. Firstly, the wave propagation in the transmission-line network should mimic the wave propagation in free space, i.e., the wave propagation should be isotropic and lie on the same dispersion curve as that in free space. If this precondition is not satisfied, the cloak will scatter. Secondly, the transmission-line network should be impedance-matched to free space in order to prevent reflections from the cloak. The impedance matching includes also the requirement that there exists a transition layer around the cloak which couples the waves propagating in free space into the network. This transition layer can be realized, e.g., with an antenna array.

III. Dispersion and Impedance in Loaded and Unloaded Transmission-Line Networks

To study the propagation inside a transmission-line network, we first derive the dispersion equations for loaded transmission-line networks, where the lumped loads are defined only as series impedance Z and shunt admittance Y. Here we can use the same derivation procedure as in [12] for a three-dimensional loaded transmission-line network, where the loads were defined as $Z = 1/(j\omega C)$ and $Y = 1/(j\omega L)$, C and L being the capacitance and inductance of the lumped loads. The dispersion equation for a 3D case with arbitrary loads Z and Y reads

$$\cos(k_x d) + \cos(k_y d) + \cos(k_z d) = \frac{Y}{2S} - 3\frac{K}{S} \tag{1}$$

and for the 2D case

$$\cos(k_x d) + \cos(k_y d) = \frac{Y}{2S} - 2\frac{K}{S} \tag{2}$$

where

$$S = \frac{Z}{(ZA_{TL} + B_{TL})(ZD_{TL} + B_{TL}) - B_{TL}^2} \tag{3}$$

$$K = \frac{Z(A_{TL}D_{TL} - B_{TL}C_{TL})(ZA_{TL} + B_{TL})}{[(ZA_{TL} + B_{TL})(ZD_{TL} + B_{TL}) - B_{TL}^2]\,B_{TL}} - \frac{A_{TL}}{B_{TL}} \tag{4}$$

$$\begin{bmatrix} A_{\rm TL} & B_{\rm TL} \\ C_{\rm TL} & D_{\rm TL} \end{bmatrix} = \begin{bmatrix} \cos(k_{\rm TL}d/2) & jZ_{\rm TL}\sin(k_{\rm TL}d/2) \\ jZ_{\rm TL}^{-1}\sin(k_{\rm TL}d/2) & \cos(k_{\rm TL}d/2) \end{bmatrix} \tag{5}$$

k_i is the wavenumber in the network along axis i, d is the period and $k_{\rm TL}$ and $Z_{\rm TL}$ are the wavenumber and impedance of the transmission lines, respectively. The wavenumber in the network is $k = \sqrt{k_x^2 + k_y^2 + k_z^2}$.

Obviously the simplest two-dimensional transmission-line network is an unloaded one. The dispersion equation for an unloaded network is obtained by using (2) and choosing $Z = 0$ and $Y = 0$. We have chosen the dimensions and impedance values for the unloaded network in such a way that the impedance of the network is approximately equal to the free space impedance, i.e., 377 Ω, at frequency $f = 1$ GHz. See Table I for the parameters of the unloaded network (k_0 is the free space wavenumber) and Fig. 2 for the plotted dispersion curves for axial and diagonal propagation. From Fig. 2 it is clear that the phase velocity $v_{\rm phase} = \omega/k$ in the network slightly differs from that in free space (light line) for $k > 0$.

TABLE I
Transmission-Line Network Parameters

-	d	$k_{\rm TL}$	$Z_{\rm TL}$	C
Loaded TL	8 mm	k_0	755 Ω	2.5 pF
Unloaded TL	8 mm	k_0	535 Ω	-

A capacitively loaded transmission-line network can be designed in such a way that its phase velocity equals that in free space for a given frequency point. This can be done, e.g., by choosing $Z = 1/(j\omega C)$ and $Y = 0$ in (2). We have designed this network in such a way that the propagation in the network and the impedance of the network are matched with free space at $f = 1$ GHz. See Table I for the parameters of this capacitively loaded network and Fig. 2 for the plotted dispersion curves.

The required isotropy of the networks is achieved if the period is small compared to the wavelength. From Fig. 2 we can

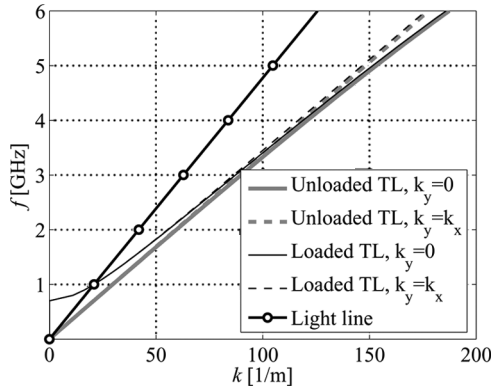

Fig. 2. Dispersion in unloaded and loaded transmission-line networks for axial and diagonal propagation.

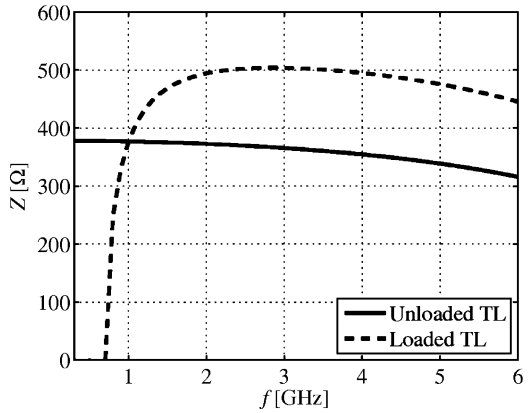

Fig. 3. Impedances of the networks, calculated for axial propagation.

conclude that for the presented designs the isotropy is achieved for both networks approximately below 3 GHz. In Fig. 3 the impedances of the two studied networks are calculated using the equations for the network impedances derived in [12].

From the above discussion, we can conclude that the both types of networks have certain benefits and drawbacks. Although the phase velocity can be ideal for the loaded network, the group velocity is smaller than the speed of light. This means that the loaded network has the same restriction of cloaking from time-harmonic fields only as, e.g., the designs in [1]–[4]. On the other hand, in the unloaded network, the phase velocity equals the group velocity. This enables cloaking from signals. However, the phase and group velocities are not ideal since they do not equal to those in free space. In the rest of this paper, we will concentrate on studying the unloaded network, due to the possibility of signal operation and inherently larger bandwidth. The larger bandwidth is expected due to the linear dispersion of the unloaded network. First, we will study the effect of the aforementioned non-ideal phase velocity on cloaking and then present a simple way of matching the unloaded network with free space.

It must be noted though, that the non-ideal phase velocity inherent to the unloaded network is a problem mostly when cloaking objects that are placed in free space. If the background material has a refractive index n equal to (or higher than) $\sqrt{2}$, it is possible that inside the transmission-line sections the wave travels faster than in the background material (e.g., if $k_{\mathrm{TL}} = k_0$) and therefore cancels out the reduction of the phase velocity in the network.

IV. Effect of Non-Ideal Phase Velocity on Cloaking

A. Scattering From the Cloak

To be able to study the effect of non-ideal phase velocity (which is related only to the unloaded transmission-line cloak), we consider a cloak having ideal impedance-matching with the surrounding medium. The transmission-line network is represented as a homogeneous material with certain relative permittivity ε_r and permeability μ_r (with their ratio equal to unity, as in free space). Using (2), it can be found that this homogeneous material should have relative permittivity and permeability equal to $\sqrt{2}$. With these parameters the dispersion curve of our homogeneous material lies exactly on the dashed curve of Fig. 2 (i.e., diagonal propagation in the unloaded network). We can conclude that the homogeneous material represents the dispersion of the unloaded network very well for all propagation directions in the region where the network is isotropic. In the following, we study a cylinder made of a homogeneous material with $\varepsilon_r = \mu_r = \sqrt{2}$. The cylinder is infinite in the z-direction. The diameter of the cylinder is 128 mm. Note that here the period is not defined, for the network is modelled with a homogeneous material.

Scattering cross section [16] is one quantitative measure for the performance of an idealized cloak. Here the scattering cross section is calculated numerically using a finite element method (FEM) based COMSOL Multiphysics software. The simulation setup is the following: the scatterer is placed in the center of a cylinder coated with a perfectly matched layer (PML) and the scatterer (cloak) is illuminated with a plane wave. The geometrical symmetry allows us to cut the problem in half using a perfect magnetic conductor (PMC) boundary, see Fig. 4. From the solved simulation, the scattered field is calculated in all directions around the scatterer. The scattered far field E_s is calculated from the near field using the Stratton-Chu formula on the inner boundary of the PML [17]. The scattering cross section σ_s is obtained from the scattered far field with

$$\sigma_s(\varphi) = 2\pi R \frac{|E_s|^2}{|E_{\mathrm{inc}}|^2} \tag{6}$$

where φ is the angle, R is the distance from the center of the scatterer to the inner boundary of the PML, and E_{inc} is the incident electric field.

The scattering cross section was calculated for the idealized cloak and for an array of vertical rods made of a perfect electric conductor (PEC). The PEC rods have a cross section of 4 mm $\times$ 4 mm (a realizable cloak period has been assumed to be 8 mm) and the rods are placed in the form of a hexagonally shaped array. The PEC rod array's outer dimensions are smaller than the diameter of the simulated homogenized cloak. The PEC rods constitute the reference object that could be hidden by the cloak.

The most interesting case to study is the total scattering cross section, where the scattering cross section is integrated over the angle φ. See Fig. 5 for the total scattering of the cloak, calculated

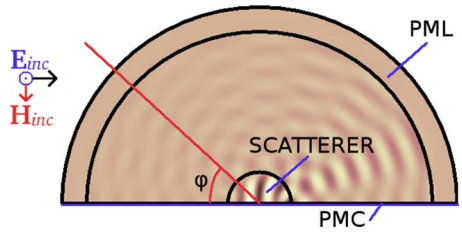

Fig. 4. Model for calculating the scattering cross section of the cloak and reference objects.

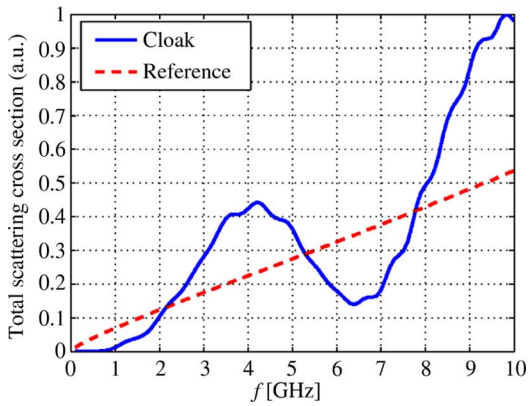

Fig. 5. Simulated total scattering cross section of the cloak and the reference object, normalized to the maximum value of the cloak's total scattering. The cloak diameter is 128 mm.

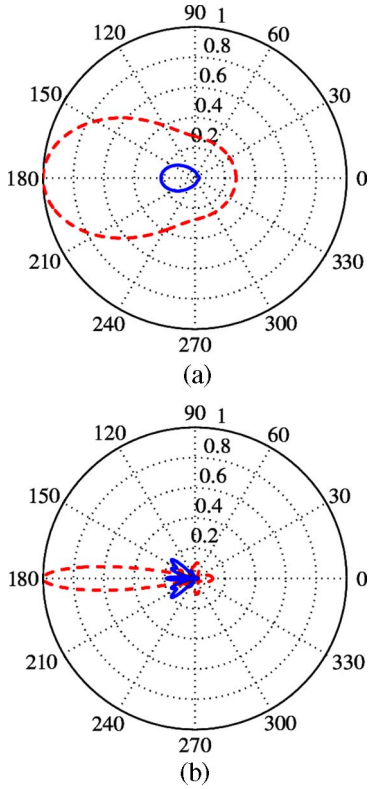

Fig. 6. Simulated scattered electric field to different directions from the cloak (solid line) and the reference object (dashed line) at frequencies (a) 1 GHz and (b) 6.4 GHz. Both plots are normalized to the maximum value of the reference object scattering. The plane wave that illuminates the cloak/reference object travels in the direction $\varphi = 180°$.

from the scattered field obtained from the simulations. Because the cloak is impedance-matched to free space, the back scattering from the (homogeneous) cloak is always below that of the reference object. From Fig. 5 we can thus conclude that for some frequencies the forward scattering from the cloak is very strong, in some directions even stronger than from the reference object. From Fig. 5 we see that the cloaking efficiency (total scattering from the cloak as compared to the reference case) fluctuates quite strongly, whereas the scattering from the reference object smoothly increases with increasing frequency. We have found that this phenomenon is due to the phase matching at the backside of the cloak. For example, at the frequency 4 GHz, the wave front at the backside of the cloak and in free space are almost in opposite phase. This leads to strong scattering from the backside of the cloak.

On the other hand, as the frequency is increased, the phase difference between the cloak edge and free space becomes smaller and reaches zero at some frequencies. Therefore the cloaking efficiency starts to improve after 4 GHz and around 6 GHz there is a band where the cloak scatters much less than the reference object. Note that good cloaking efficiency is achieved also at low frequencies, where the cloak is small compared to the wavelength. In the example case studied here, the cloak diameter should be smaller than approximately a half wavelength in order to achieve significant reduction of the total scattering cross section. The scattering from the cloak and from the reference object to different directions, at the frequencies 1 and 6.4 GHz, is plotted in Fig. 6, from which it is obvious that the backscattering from the cloak is strongly reduced and also the forward scattering is considerably lower than that of the reference object (at those specific frequencies). The reader must note that in the scattering simulations the cloak is modelled as a homogeneous material which is fully isotropic at all frequencies. For the studied transmission-line networks with period $d = 8$ mm, the isotropy is achieved approximately below the frequency 3 GHz, as discussed above. The isotropic region can be extended to higher frequencies by decreasing the period of the structure, but this has the drawback of reducing the maximum size of the cloaked object's inclusions.

B. Cloaking From Signals

To take advantage of the most promising feature of the cloak proposed in this paper, i.e., cloaking from signals, we have to use the unloaded transmission-line network. This choice has also the advantage of larger operation bandwidth, due to the linear dispersion characteristics and the slowly varying impedance, see Figs. 2 and 3. As discussed above, this choice has the drawback of non-ideal phase velocity. To obtain more information about the effect of this non-ideality on cloaking, and especially cloaking from signals, we have simulated the cloak using a finite-difference time-domain (FDTD) code. FDTD is suitable for this task, since it inherently includes the possibility of signal excitation.

In the FDTD simulations, we have modeled a cloak having the same diameter as the homogeneous cloak studied above. The diameter of the cylindrical cloak is therefore $16d = 128$ mm and the period of the interconnecting transmission lines is 8 mm.

The cloak has the same dispersion as shown in Fig. 2 (unloaded network). The FDTD code takes into account the anisotropy that occurs at the higher frequencies. To study only the effect of non-ideal dispersion, we have ideal impedance-matching between the cloak and free space. As a reference object, we again have a mesh of PEC wires, placed in the position of the cloak. The PEC wires form a cylindrically shaped mesh that fits inside the studied cloak. The cloak and the reference object are excited by a signal with vertically polarized electric field, i.e., $\overline{E}$ is oriented along the z-axis.

According to Fig. 5, we can expect good cloaking (as compared to the reference object) at frequencies below 2 GHz, and, e.g., in the band from 5.5 to 7.5 GHz. See Fig. 7 for the simulation results for pulses with center frequencies at 1, 2, and 5.5 GHz. In Fig. 7 snapshots of the electric field distributions are taken at a time step when the signal has just passed the cloak/reference object, i.e., the signal comes from the left and moves to the right in Fig. 7. The signal bandwidths used in the FDTD simulations are relatively large: in Fig. 7(a), (b) the relative half-power pulse width is 52% with center frequency $f_c = 1$ GHz, in Fig. 7(c), (d) it is 26% with center frequency $f_c = 2$ GHz and in Fig. 7(e), (f) it is 9.5% with center frequency $f_c = 5.5$ GHz.

From Fig. 7 we see that at all the shown frequencies, the backscattering from the cloak is zero, and that inside the cloak, the waves are "delayed," with respect to the waves propagating in free space (this is due to the shorter wavelength inside the cloak). Because of this, some forward scattering from the cloak occurs, although the shadow generated by the cloak is always well mitigated, as compared to the reference object. The FDTD simulations seem to confirm the cloaking effect, studied for the time-harmonic case in Fig. 5, also for signal excitation. The pulse with center frequency of 5.5 GHz, presented in Fig. 7(e), (f) is already at the frequency range where the network is anisotropic. The transmission-line network in FDTD simulations is not capable of supporting higher frequencies, because the wavelength becomes too short compared to the period of the network. Despite of the anisotropy, Fig. 7(f) demonstrates the benefit of the phase matching inside and outside the cloak: because the waves that emerge from the backside of the cloak are in phase with the waves outside the cloak, the wavefronts at the back of the cloak prevent the formation of a strong shadow.

It is clear that the best cloaking effect (cloak scattering versus the reference object scattering) is always achieved at low frequencies. The phase matching technique can be used if the cloak must be large compared to the wavelength.

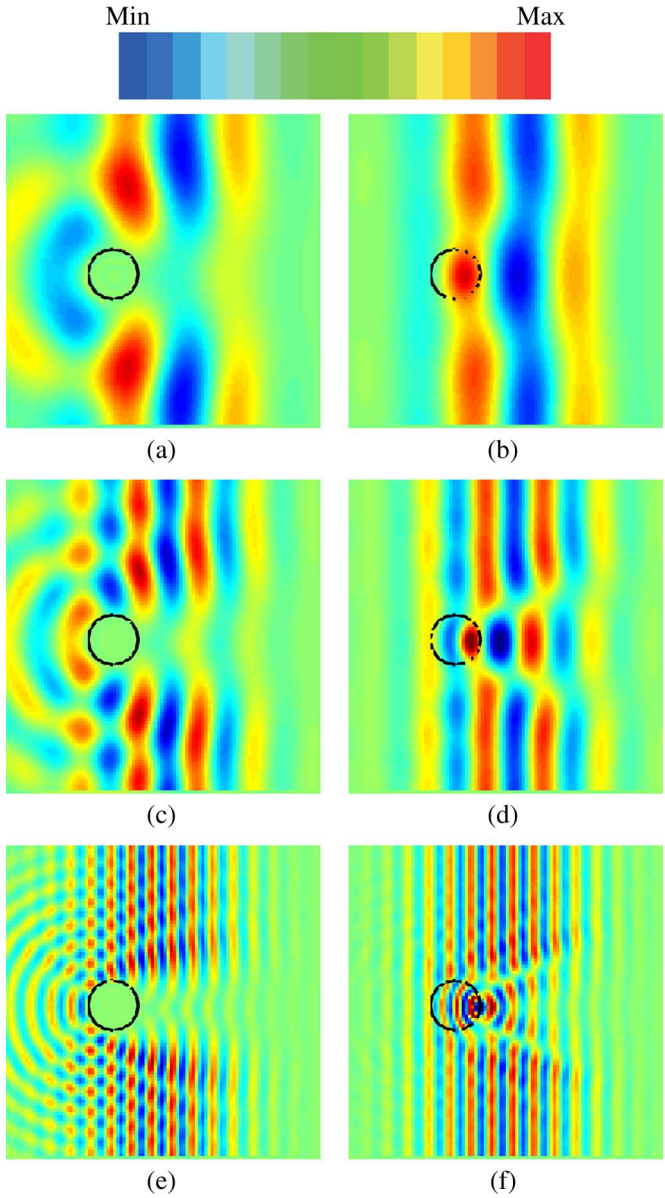

Fig. 7. Color Online. Electric field snapshots from FDTD simulations (all normalized to the same amplitude value). (a) Reference object, $f_c = 1$ GHz. (b) Cloak, $f_c = 1$ GHz. (c) Reference object, $f_c = 2$ GHz. (d) Cloak, $f_c = 2$ GHz. (e) Reference object, $f_c = 5.5$ GHz. (f) Cloak, $f_c = 5.5$ GHz.

V. Simulation of a Realizable Cloak

In this section we present a simple way of matching the transmission-line network to free space. Furthermore, we verify the operation of the cloak by full-wave simulations using Ansoft's High Frequency Structure Simulator (HFSS). The previous section of this paper was devoted to study of the non-ideal propagation characteristics of the unloaded network while assuming perfect impedance matching between the cloak and the surrounding medium. In this section we first study a transversally infinite slab made of two-dimensional unloaded transmission-line networks, thus effectively studying only the transition from free space to the cloak and vice versa. The reader should notice here that unlike in the previous section, the thickness of the transversally infinite slab does not have any effect on the phase matching between the waves travelling inside and outside of the cloak. However, since the wavelength inside the slab differs from that in free space we expect to see Fabry-Perot type resonances in the reflection and transmission coefficients due to the finite electrical length of the slab (along the x-axis). In the end of this section we present simulation results also for a slab with finite width in order to give some further demonstration of the cloaking capabilities.

The use of periodical boundary conditions allows us to simplify the simulation model of the transversally infinite slab: We need to model only one "unit cell" of the slab as shown in Fig. 8.

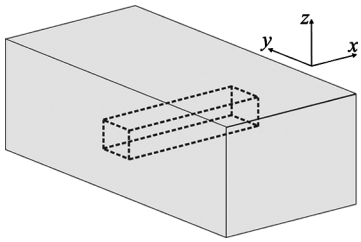

Fig. 8. Modelled slab made of two-dimensional transmission-line networks which are placed on top of each other. The slab is infinite in the y- and z-directions. The dashed line shows a single "unit cell" of the slab, which can be easily modelled with full-wave simulators using periodic boundaries.

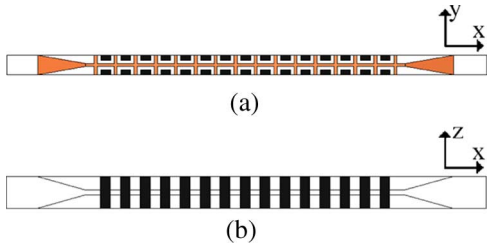

Fig. 9. HFSS model of the cloak with reference object inside (a) viewed from the top and (b) viewed from the side. The reference object is illustrated with black color.

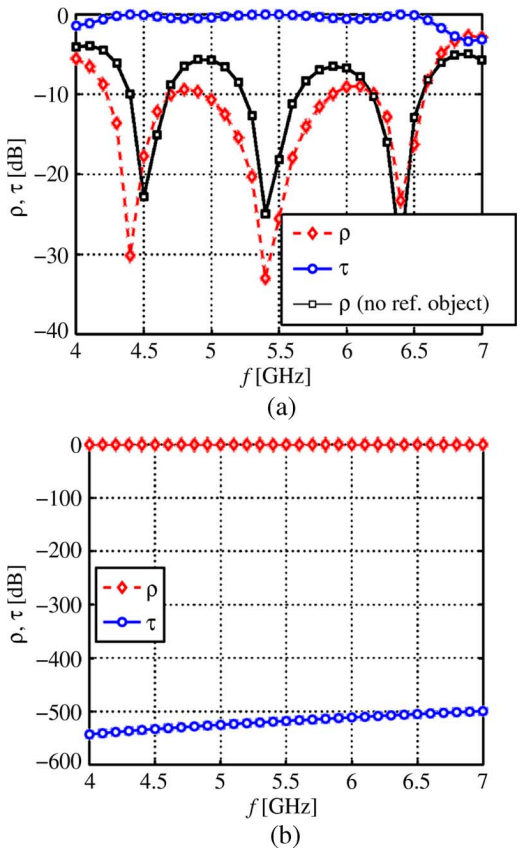

Fig. 10. Simulated reflection and transmission for (a) cloak slab with reference object inside and (b) reference object. A plane wave illuminates the cloak slab with normal incidence.

The slab shown in Fig. 8 is infinite in the y- and z-directions, but along the x-axis it is finite with thickness of $16d = 128$ mm.

Based on the simulated scattering and the FDTD results presented in the previous section, we have decided to tune the network impedance in order to obtain the impedance matching at higher frequencies (above 5 GHz), see Fig. 5. This is because it is obvious that at lower frequencies (i.e., when the cloaked object is small compared to the wavelength) the scattering can be greatly reduced with the cloak, but the main advantage of the cloak design proposed in this paper is cloaking from signals, which is more problematic with objects that have sizes comparable to the wavelength.

To obtain impedance matching at higher frequencies, the impedance of single sections of transmission lines should be increased to raise the curve shown in Fig. 3, in order to obtain the impedance of 377 Ω at a frequency above 5 GHz. Using the impedance equations from [12] we have found that the transmission-line impedance of 600 Ω results in the network impedance of 377 Ω at approximately 5.2 GHz. As the transmission lines, we have chosen to use parallel metal strips due to the large range of impedance values available and the simple geometry and easy manufacturing of this type of transmission line. Using the simple parallel-plate approximation, we have calculated the width w and height h of the transmission line to be 1.257 mm and 2 mm, respectively. The metal strips are modelled as infinitely thin and perfectly conducting to reduce the simulation time.

Matched transition from free space to the cloak and vice versa can be obtained by extending the transmission lines at the both sides of the cloak, while preserving the impedance of the transmission lines. This way the both slab surfaces are covered with small sections of transmission lines, effectively operating as antennas with their input impedance equal to the free space impedance. See Fig. 9 for the HFSS simulation model of the "unit cell" of the slab.

As shown in Fig. 9, the antennas cover almost all of the area of the unit cell in the yz-plane, but in fact, there is a tiny gap left between the antennas of the neighboring unit cells (approximately 2 μm in the z-direction and 120 μm in the y-direction). The width and height of the simulated unit cell are 8 mm and 12.73 mm, respectively, to preserve the correct impedance of the transmission lines ($12.73/8 \approx 2/1.257$). We have also placed a reference object that we want to cloak, inside the network, see Fig. 9. This reference object is an array of rods made of PEC, as in the scattering simulations. The rods have a cross-section of 4 mm × 4 mm and they are effectively infinite along the z-axis.

The cloak is excited with a plane wave having the electric field parallel to the z-axis. First, we have studied the case of the normal incidence angle (magnetic field $\overline{H}$ is parallel to the y-axis). See Fig. 10(a) for the simulated reflection (ρ) and transmission (τ) coefficients for the cloak with the reference object inside and Fig. 10(b) for ρ and τ in the case of the reference object only.

From Fig. 10 it is obvious that the reference object behaves effectively as a solid metal slab reflecting basically all of the incident field, whereas the same object placed inside the cloak is almost transparent to the incident field. We believe that the resonances seen in the reflection and transmission through the cloak are due to the finite thickness of the cloak, as discussed

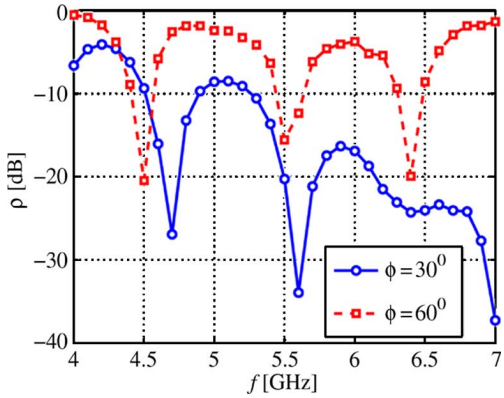

Fig. 11. Simulated reflection coefficients for the cloak with reference object inside. Oblique incidence angles of $\phi = 30°$ and $\phi = 60°$ are considered.

above. The minimum of the envelope of the reflection coefficient in Fig. 10(a) occurs at approximately 5.4 GHz, which is close to the expected value of 5.2 GHz, obtained from the analytical expressions for the network impedance.

In addition, we have made simulations of the cloak slab without the reference objects inside, in order to demonstrate that the properties of the cloaked object do not change the properties of the cloak dramatically. Of course, since in our example case the transmission lines are composed of parallel strips, there are some fringing fields near the lines and the cloaked object affects somewhat the propagation characteristics. See Fig. 10(a) for this case, from which it can be concluded that the minima of the reflection occur approximately at the same frequencies with and without the reference object. In the simulation model without the reference object, we have added PEC plates with a small hole in the center, positioned in the yz-plane at the interconnections between the antennas and the strips, in order to prevent unwanted modes (modes that do not travel between the strips) from entering the network. The introduction of these PEC plates also explains the difference in the envelopes of the reflection curves with and without the reference objects.

The effect of oblique incidence angle was also considered for two cases: $\phi = 30°$ and $\phi = 60°$, where ϕ is the angle in the xy-plane, i.e., the electric field $\overline{E}$ is always directed along the z-axis. See Fig. 11 for the simulation results of the reflection coefficient ρ as a function of the frequency for these two incidence angles.

Note that the positions of the resonance frequencies seen in the reflection coefficient are affected by the oblique incidence due to the shift in the Fabry-Perot resonances: the effective thickness of the slab changes as the incidence angle changes. At frequencies above 3 GHz the transmission-line networks studied in this paper are anisotropic, which also changes the electrical thickness of the slab for different incidence angles. Nevertheless, for the frequencies 5.5 and 6.4 GHz, the reflection coefficient remains very low for all the studied incidence angles.

In order to demonstrate the robustness of the current approach to match the transmission-line network to free space, we have made simulations of the same type of cloak slab as above, but with a finite size in the y-direction. By making a finite simulation model, we can excite the structure with, e.g., a cylindrical wave to have clear variation of the incidence angle of the incoming wave with respect to the cloak. The HFSS simulation results of the time-harmonic electric field at 5.5 GHz, for a cloak slab with a finite size (32×8 unit cells) in the xy-plane and the corresponding reference case, are shown in Fig. 12. From Fig. 12(a) it is obvious that the incoming cylindrical wave couples to the cloak and inside the cloak the waveform is nicely preserved. Some distortion of the field occurs at the backside of the cloak simply because of the strong scattering from the edges of the slab. In the case of the reference object, most of the incoming wave is scattered back from the object, see Fig. 12(b).

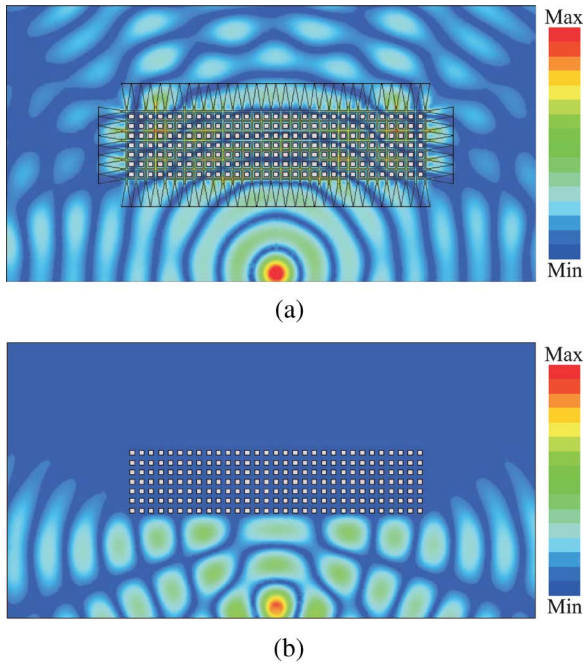

Fig. 12. Snapshots of the simulated time-harmonic electric field at 5.5 GHz (a) for a finite cloak slab with the reference object inside and (b) for the reference object.

To further demonstrate the quality of matching, we have simulated the phase of the electric field in the situation discussed above. See Fig. 13 for the phase distributions corresponding to the same cases as presented in Fig. 12.

VI. Conclusion

We have shown that transmission-line networks can be used to cloak objects from electromagnetic fields. The inclusions of an object that can be cloaked have to be smaller than the period of the cloak itself, which is composed of either loaded or unloaded transmission-line networks. The propagation characteristics of the transmission-line network have to mimic the propagation in the medium that surrounds the cloak. If this medium is free space, the optimal propagation characteristics of the cloak cannot be achieved with an unloaded network. A periodically loaded transmission-line network on the other hand can be designed to have ideal propagation characteristics, but the operation of this cloak is very narrowband and it suffers from similar non-idealities as the cloak designs presented in the literature. The unloaded transmission-line networks seem to be more

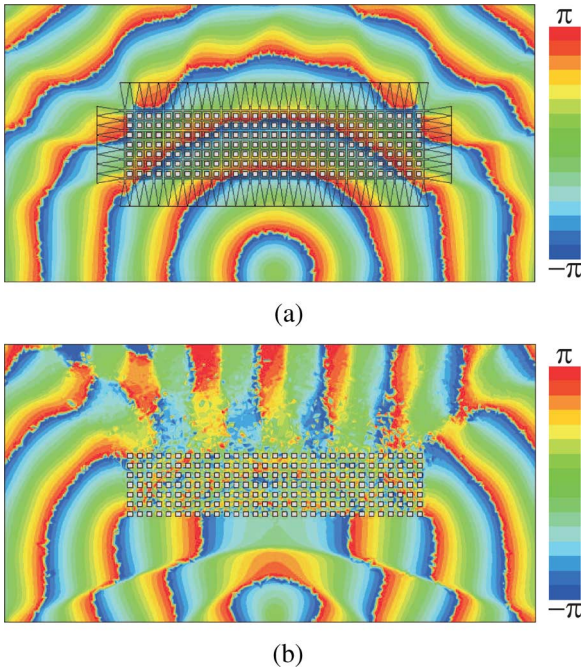

Fig. 13. Simulated electric field phase at 5.5 GHz (a) for a finite cloak slab with the reference object inside and (b) for the reference object.

prospective for applications that require simple manufacturing and large bandwidth.

We have thoroughly studied the effect of non-ideal propagation characteristics on cloaking and have shown that when the cloak is small enough as compared to the wavelength, good cloaking efficiencies are achieved. Also, at higher frequencies the cloaking effect is achieved at frequencies that depend on the physical size of the cloak. This is due to the phase matching of the wave at the backside of the cloak and the wave in the surrounding medium. We have shown how a realizable transmission-line network can be matched to free space and have presented full-wave simulations for a slab made of such a network placed in free space.

ACKNOWLEDGMENT

This work was initially started as a student project work at the TKK Radio Laboratory and the TKK Electromagnetics Laboratory within a postgraduate course "Metamaterials in Electromagnetics and Radio Engineering." The authors wish to thank A. Karttunen, G. Molera, H. Rimminen, M. Vaaja and Prof. A. Sihvola for useful discussions during that course. The authors also wish to thank J. Vehmas for valuable help with the simulations.

REFERENCES

[1] U. Leonhardt, "Optical conformal mapping," *Science*, vol. 312, pp. 1777–1780, 2006.

[2] J. B. Pendry, D. Schurig, and D. R. Smith, "Controlling electromagnetic fields," *Science*, vol. 312, pp. 1780–1782, 2006.

[3] W. Cai, U. K. Chettiar, A. V. Kildishev, and V. M. Shalaev, "Optical cloaking with non-magnetic metamaterials," *Nature Photon.* vol. 1, pp. 224–227, 2007.

[4] D. Schurig, J. J. Mock, B. J. Justice, S. A. Cummer, J. B. Pendry, A. F. Starr, and D. R. Smith, "Metamaterial electromagnetic cloak at microwave frequencies," *Science*, vol. 314, pp. 977–980, 2006.

[5] A. Alù and N. Engheta, "Achieving transparency with plasmonic and metamaterial coatings," *Phys. Rev E*, vol. 72, p. 016623, 2005.

[6] A. Alù and N. Engheta, "Plasmonic materials in transparency and cloaking problems: Mechanism, robustness, and physical insights," *Opt. Expr.*, vol. 15, no. 6, pp. 3318–3332, 2007.

[7] M. G. Silveirinha, A. Alù, and N. Engheta, "Parallel-plate metamaterials for cloaking structures," *Phys. Rev E*, vol. 75, p. 036603, 2007.

[8] G. W. Milton and N. A. Nicorovici, "On the cloaking effects associated with anomalous localized resonance," *Proc. R. Soc. Lond. A: Math. Phys. Sci.*, vol. 462, pp. 3027–3059, 2006.

[9] P.-S. Kildal, A. A. Kishk, and A. Tengs, "Reduction of forward scattering from cylindrical objects using hard surfaces," *IEEE Trans. Antennas Propag*, vol. 44, no. 11, pp. 1509–1520, 1996.

[10] C. Caloz, H. Okabe, T. Iwai, and T. Itoh, "Transmission line approach of left-handed (LH) materials," in *Proc. USNC/URSI National Radio Science Meeting*, San Antonio, TX, Jun. 2002, vol. 1, p. 39.

[11] G. V. Eleftheriades, A. K. Iyer, and P. C. Kremer, "Planar negative refractive index media using periodically $L - C$ loaded transmission lines," *IEEE Trans. Microw. Theory Tech.*, vol. 50, no. 12, pp. 2702–2712, Dec. 2002.

[12] P. Alitalo, S. Maslovski, and S. Tretyakov, "Three-dimensional isotropic perfect lens based on LC-loaded transmission lines," *J. Appl. Phys.*, vol. 99, p. 064912, 2006.

[13] A. Grbic and G. V. Eleftheriades, "An isotropic three-dimensional negative-refractive-index transmission-line metamaterial," *J. Appl. Phys.*, vol. 98, p. 043106, 2005.

[14] W. J. R. Hoefer, P. P. M. So, D. Thompson, and M. M. Tentzeris, "Topology and design of wide-band 3D metamaterials made of periodically loaded transmission line arrays," in *Proc. IEEE MTT-S Int. Microwave Symp. Digest*, Jun. 2005, pp. 313–316.

[15] M. Zedler, C. Caloz, and P. Russer, "Circuital and experimental demonstration of a 3D isotropic LH metamaterial based on the rotated TLM scheme," in *Proc. IEEE MTT-S Int. Microwave Symp. Dig.*, Honolulu, HI, Jun. 2007, pp. 1827–1830.

[16] A. F. Peterson, S. L. Ray, and R. Mittra, *Computational Methods for Electromagnetics*. New York: IEEE Press, 1998.

[17] Y. T. Lo and S. W. Lee, *Antenna Handbook, Theory, Applications and Design*. New York: Van Nostrand Reinhold Company, 1988.

Pekka Alitalo was born on July 20, 1981, in Tammela, Finland. He received the M.Sc. degree (with distinction) in electrical engineering from the Helsinki University of Technology, Helsinki, Finland, in 2006, where he is currently working towards the D.Sc. degree.

Since 2003, he has been a Trainee, Research Assistant, and Research Engineer with the Radio Laboratory, Helsinki University of Technology. His current research interests include sub-wavelength imaging devices and novel applications of artificial transmission lines.

Mr. Alitalo is a member of the Finnish Graduate School of Electronics, Telecommunications, and Automation (GETA).

Olli Luukkonen was born on November 8, 1980, in Helsinki, Finland. He received the M.Sc. degree in electrical engineering from the Helsinki University of Technology in 2006, where he is currently working towards the D.Sc. degree.

Since 2005, he has been working as a Research Assistant and Research Engineer with the Radio Laboratory, Helsinki University of Technology. His current research interests include artificial impedance surfaces and their applications.

Liisi Jylhä was born on May 4, 1979, in Finland. She received the M.Sc. degree and the Lic. Tech. in electrical engineering from the Helsinki University of Technology, Finland, in 2003 and 2005, respectively, where she is currently working towards the D.Sc. degree.

Her current research interests include numerical and analytical modeling of composite materials.

Ms. Jylhä is funded by the Finnish Graduate School of Electronics, Telecommunications, and Automation (GETA).

Jukka Venermo was born on May 7, 1980, in Kerava, Finland. He received the M.Sc. degree (with distinction) in electrical engineering from the Helsinki University of Technology, Helsinki, Finland, in 2007, where he is currently working towards the D.Sc. degree.

Since 2002, he has been a Trainee, Research Assistant, and Research Engineer in the Electromagnetics Laboratory, Helsinki University of Technology. His current research interests include modeling of artificial electromagnetic materials.

Sergei A. Tretyakov (M'92–SM'98–F'08) received the Dipl. Engineer-Physicist, the Candidate of Sciences (Ph.D.), and the Doctor of Sciences degrees, all in radiophysics, from the St. Petersburg State Technical University, Russia, in 1980, 1987, and 1995, respectively.

From 1980 to 2000, he was with the Radiophysics Department of the St. Petersburg State Technical University. Presently, he is a Professor of radio engineering in the Radio Laboratory, Helsinki University of Technology, Espoo, Finland, and coordinator of the European Network of Excellence *Metamorphose*. His main scientific interests are electromagnetic field theory, complex media electromagnetics and microwave engineering.

Prof. Tretyakov served as Chairman of the St. Petersburg IEEE ED/MTT/AP Chapter from 1995 to 1998.